https://doi.org/10.20965/ijat.2014.p0880

Paper:

Research on the Form Recognition of Fabric Products: Acquiring the Shapes of Flat, Limp Materials

Fumiaki Osawa, Kazunori Kanou, and Yasushi Yamada

Department of Electrical and Electronic Engineering, Daido University
10-3 Takiharu-cho, Minami-ku, Nagoya 457-8530, Japan
E-mail: osawa@daido-it.ac.jp

[Received April 6, 2014; accepted July 8, 2014]

In the apparel, medical and welfare, and nursing care industries, working with cloth items is highly dependent on manual work, so many people have hoped that such work could be automated. However, there are still no established ways for robots to handle cloth. In this paper, a method for acquiring developed shapes is proposed for the purpose of form recognition and classification operations of flat, limp materials. Experiments are performed to acquire developed shapes of materials by actively searching for contours of cloth using a sensor embedded in the finger of a robot.

Keywords: limp materials, contour shape, image sensor, recognition

1. Introduction

In the clothing and textile field as well as at manufacturing sites, working with limp materials is highly dependent on manual work, and it has been hoped that such work could be automate. In addition, in the nursing care as well as medical and welfare industries, expectations have been raised for human support robots that can sophisticatedly handle objects of various shapes, such as garments and linens. On the other hand, the properties of cloth differ with the fiber, thread formation methods, sheet weaving methods, and processing methods. It is difficult to anticipate shapes, forms, and dynamic deformations of cloth because the properties of cloth in terms of material mechanics such as bend, shear, expansion, and thickness are non-linear and anisotropic in many cases. Technologies for handling and recognizing cloth items have therefore not been established.

Research studies done on handling cloth have been related mainly to automatic sewing systems. Devices dedicated to moving cloth, ones that raise a flat piece of cloth and place it in a horizontal position, have been reported [1–5]. An attempt to utilize sensing information for robots to handle cloth has also been reported [6]. In addition, a method of plane development involving calculating the positions of corner edges of cloth folded in a plane and using a vision sensor to pick up cloth has been proposed [7]. As an automation project for a commercial laundry, a system was devised that uses a stereo camera and pattern projector to detect the corners of towels and sheets to pick them up and throw them into a machine [8]. A cloth development system that detects the edges of a piece of cloth using an infrared sensor installed in a robot hand has been proposed [9]. Using high-speed multiple fingers and sliders to dynamically fold cloth has been proposed [10]. These examples handled rectangular pieces of cloth. Regarding the handling of garments, in an ongoing project, the positions for gripping developed clothes have been calculated by representing hanging garments using a multi-mass model and predicting changes in shape [11]. A method of calculating grip positions was proposed in order to grasp an article of clothing from a pile of laundry [12]. A way of using a GUI operation to teach how to fold clothes was proposed as part of the theme of a movable robot that folds clothes on a floor [13].

Concerning recognizing the forms of clothes, a method for making out certain types of clothes has been developed. The method involves calculating geometric feature quantities of shapes of clothes [14]. Furthermore, a method has been developed for classifying clothes in a converged shape by passing them hanging from one dual arm to the other [15]. However, it was difficult to calculate the grip points or recognize their forms when the clothes were in contact with a floor or when parts were folded and hidden out of the camera's field of vision. A large work space was also required for the clothes to be spread out.

The goal of this research is to formulate a small-scale cloth handling system for use in nursing care facilities or ordinary houses, a system that can recognize forms and classify flat, limp materials, such as clothes, in complicated shapes. The fact that cloth may be in contact with the floor or candidate points for gripping may be hidden from the camera's field of vision should be assumed. A technology for actively seeking out grip points and being able to recognize and classify clothes without first spreading them completely out is required. This paper proposes a method for acquiring developed and corrected shapes of materials by actively using the fingertips of the robot to find the edges of garments or other items made of cloth.

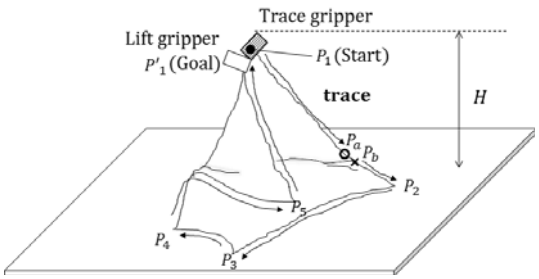

Fig. 1. Tracking the contour flat, limp materials.

2. Foam Acquisition through Contour Tracing

This paper deals with pieces of cloth with straight or contoured edges being classified by item, such as by the article of clothing it is, based on its shape or size.

Figure 1 shows the concept of acquiring contour information by tracing the contours of an object. In the initial condition, one hand, hereinafter referred to as the "hanging hand," lifts the object to a point adjacent to the corner edge P_1 while the other hand, hereinafter referred to as the "tracing hand," pinches it at P_1. An image sensor embedded in the finger of the tracing hand acquires local contour images of the object it is pinching. Chain coding is performed by extracting from the local contour images the pixel rows that constitute contours. Successive contour information is obtained by tracing the edge of the object, lightly pinching it with the fingertips. The chain code from the starting point to the end of the contour tracing is mapped to the coordinate of pixel rows to acquire the contour shape. At corner edges P_2, P_3, P_4, and P_5, where the curvature significantly changes, the object might be deformed owing to considerable changes in the direction of the tracing motion. The tracing hand, therefore, traces the contour up to P_2 and then passes over P_2 to the hanging hand before tracing the contour up to P_3. Here, the passing of an object from the tracing hand to the hanging hand is defined as the "regrasping motion." All contours are traced by repeating the tracing motion and the regrasping motion at points where the curvature changes significantly with respect to the starting point P_1. When a part of the contour comes in contact with the floor and the movement of the tracing hand is restricted, the hanging hand lifts the object to avoid the restriction. When the motion range H is restricted in the vertical direction of the hanging hand, the contour up to P_a that is not in contact with the floor is traced, and then the contour from P_b to P_2 is lifted to the motion range using the hanging hand.

In this method, developed shapes of a folded object can be acquired even when a certain part (e.g., the edge of a corner) is hidden, and the cloth can be handled in a small space because an object need not be completely developed. In this paper, the problem to be solved is the acquisition of shapes by tracing local contour images.

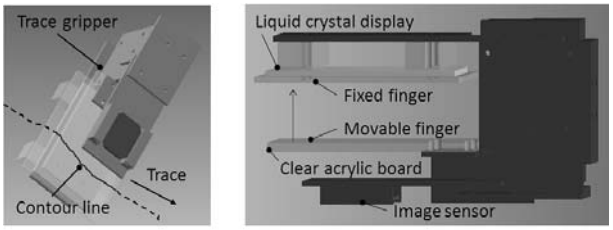

Fig. 2. Gripper for contour tracing.

3. Sensor System

3.1. System Configuration

Contours are traced using two vertically articulated, 6-DOF robot arms [16]. Images of the tracing hand can be seen in **Fig. 2**. The fingertip of the hand is composed of a movable finger and a fixed one. The open and close stroke is 33 mm. A 100×65 mm liquid crystal display providing uniform luminance is installed on the back of the fixed finger. A CMOS image sensor with a minimum local length of 20 mm that takes 640×480 pixel images is placed behind the movable finger. The sensor is fixed to the main part of the hand and does not move with the opening and closing of the finger tip. When the hand is closed, the working distance of the sensor is 55 mm, the shooting range is 97×47 m, and the resolution is 0.075 mm. Image processing calculations are performed by a computer with a 3.2 GHz Intel Core i5 CPU for the gray image over the grip range input from the sensor. The open-close width of the hand is controlled by pulse commands at a resolution of 0.00049 mm/pulse. A 6-axis haptic capacitance sensor was added to the wrist of the robot arm. The sensor measures tension when contours slip off the hands in order to monitor whether or not an object is caught on the fingers and to adjust the grip width. The maximum open-close stroke of the hanging hand is 100 mm. Its fingertip has rotational freedom, as it is driven by DC servo motors and can adjust the posture of the hanging object.

3.2. Contour Tracing Motions

A conceptual diagram for the local contour image acquired by pinching object edges with the fingertips of hands is shown in **Fig. 3**. The gray area is the gripped object, the white area the background, and the border from P_1 to P_m is the contour of the object. If the hand coordinate system is assumed to be $\sum_h$, the distance from p_k, where the Z_h axis of $\sum_h$ intersects the contour of the object, to the fingertips is defined as the grip depth.

The basic movements of the contour tracing arms are the following motion 1 and motion 2.

Motion 1: (grip depth) In order to keep an object from separating from the hands, the target positional deviation in the camera coordinate system $\sum_c$ is determined using the following equation:

$$^{c}\boldsymbol{r} = [g_h - g_h^{ref},\ 0, 0]^T \quad \ldots\ldots\ldots\ldots (1)$$

The grip depth g_h is adjusted to the target grip depth g_h^{ref}.

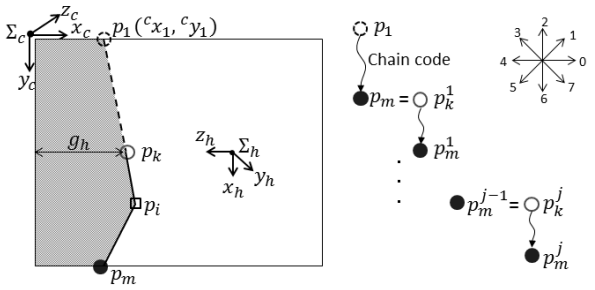

Fig. 3. Concept of local contour image and connection of local contour information.

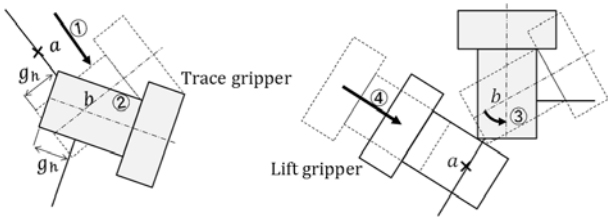

Fig. 4. Regrasping motion of dual arm.

Motion 2: (movement) The target positional deviation of the arm in $\sum_c$ is determined using the following equation:

$$ {}^{c}\boldsymbol{r} = [{}^{c}x_m - {}^{c}x_k,\ {}^{c}y_m - {}^{c}y_k, 0]^T \quad \ldots\ldots (2) $$

Hands move in the direction connecting contour pixels of P_k and P_m, and they trace the contour. Here, P_k and P_m are points where the contour line contacts the upper and lower ends of the y_c axis, respectively.

The hands trace object contours by repeating motion 1 and motion 2. Note that the object comes off the fingertips when the direction of the hand on the Z_h axis makes an acute angle with the tangential direction of the contour. In that case, the posture of the hand is controlled so that its direction is perpendicular to the tangential direction of the contour. The grip width is adjusted to satisfy the following equation:

$$ g_w > c_{th} \quad \ldots\ldots\ldots\ldots\ldots\ldots (3) $$

Here, g_w is the grip width of the tracing hand, while c_{th} is the thickness of the cloth being traced.

Figure 4 shows the regrasping motion of the arm. The tracing hand moves to point b and lifts the cloth. Then, the hanging hand regrasps cloth at the point a, adjacent to point b. The contour might not be gripped even with the maximum grip width of the hanging hand when a large portion is folded at point a. The posture of the tracing hand Θ is, therefore, controlled so that the contour at point is suspended linearly.

3.3. Image Processing for Local Contours

In general, the edge position where contours are formed is defined using the derivative peak value of gray-level distribution. **Fig. 5** shows the gray-level distribution in

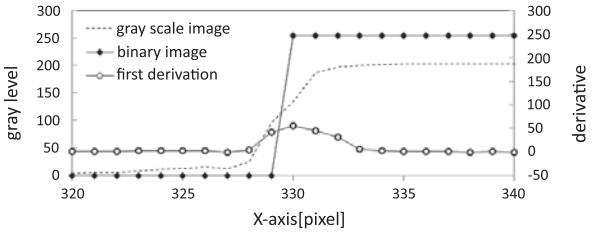

Fig. 5. Gray-level distribution of cloth contour and edge.

the perpendicular direction along with the first derivation values of gray level and the gray-level distribution of the binary image of a piece of 60% wool and 40% rayon cloth 1.8 mm thick. Because the peak position of first derivation of gray level is approximately the same as the border position of the binary image, this paper defines the border of an object and background in a binary image as a contour line.

In order to suppress the effects of the surface pattern of an object on contour extraction, uniform light radiating from the back of an object is captured by a sensor. The incident light on the cloth is reflected and defused on the thread surface, absorbed by the thread, transmitted through (hereinafter referred to as light transmitted through thread), or transmitted through gaps in the thread (hereinafter referred to as light transmitted through gaps). The incident light to the sensor is the light transmitted through the thread and that transmitted through gaps in it. Because the light is low in intensity, areas of the object and background can be divided by means of binarization. The threshold value of binarization is automatically determined by the discriminant analysis method. The binary image is labeled in order to remove noise from the image, and the region with the largest area is extracted as the object. By tracing border pixels between the object and background in a clockwise direction, the contour pixel row from p_1 to p_m in **Fig. 3** of $p_i({}^{c}x_i, {}^{c}y_i)\{i = 1, 2 \ldots, m\}$ is obtained to determine the chain code expressing the direction of a pixel pair. When the tracing hand moves in motion 1, P_m moves to the position P_k. This means that the entire contour is acquired by obtaining contour information from p_k^j to $p_m^j\{j = 1, 2 \ldots, n\}$ after the movement of the hand. Here, j is the order of images obtained synchronically after motion 2. In addition, with the aim of retaining connectivity of the contour line, the chain code from the starting point P_1 to the end point p_m^n is determined assuming the following:

$$ p_m^{j-1} = p_k^j $$

The entire contour shape is obtained by mapping the chain code in the coordinates of pixel rows and converting the outcome to real coordinates.

Corner edges are identified as candidates for regrasping based on contour curvature. Assuming two pixels ς pixels away from P_i along the contour line as $p_{i-\varsigma}(x_{i-\varsigma}, y_{i-\varsigma})$, $p_{i+\varsigma}(x_{i+\varsigma}, y_{i+\varsigma})$, curvature θ_i at contour pixel P_i is ex-

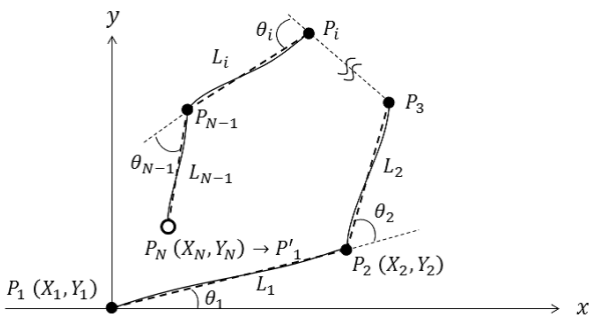

Fig. 6. Correction of contour shape by adjusting deflection angle of θ_i.

pressed as follows:

$$\theta_i = ATAN\left(\frac{y_i - y_{i-\varsigma}}{x_i - x_{i-\varsigma}}\right) - ATAN\left(\frac{y_{i+\varsigma} - y_i}{x_{i+\varsigma} - x_i}\right) \quad (4)$$

In this case, a corner edge is defined as a pixel point with the highest θ_i in the area, whereas the value of θ_i should fall within a predetermined range. Note that the value of ς is empirically determined, and multiple points with significant curvature can be detected in the case of textile looped on the surface. In such a case, the value of ς should be adjusted or $p_{i-\varsigma}$ and $p_{i+\varsigma}$ should be calculated based on average values of adjacent coordinate rows.

3.4. Form Acquisition

Figure 6 shows connected local contour lines mapped onto real plane R^2. Contour lines of an object are approximated to a polygon. Here, the number of nodes where curvature significantly changes is N, positions of nodes is $p_i(x_i, y_i)\{i = 1, 2 \ldots, N\}$, deflection angles of tangent lines at each node is $\theta_i\{i = 1, 2 \ldots, N\}$, and distance between each node is $L_i\{i = 1, 2 \ldots, N\}$.

The length of the contour line and distance between each node can be obtained at a high resolution. It is, however, difficult to eliminate deviation from actual deflection angles because θ_i is calculated based on local images. The starting point P_1 for the object contour may not correspond to the end point P_N, and the developed image to be acquired may be considerably distorted. Consequently, the deviation of deflection angles at each node is corrected by converging the starting point P_1 and the end point P_N through the adjustment of θ_i.

The position and posture at the end point P_N differ depending on the values of the deflection angles at each node. With P_1 as the origin $(0,0)$ and deflection angles at each node as $\mathbf{q} = [\theta_1, \theta_2, \ldots, \theta_{N-1}]^T$, P_N can be expressed by the following equation:

$$\boldsymbol{P}_N = \boldsymbol{f}(\boldsymbol{q}) \quad . \ . \ . \ . \ . \ . \ . \ . \ . \ . \ . \ . \ . \ . \ (5)$$

Here, using the following $2 \times N$ matrix that expresses the derivative relationship between q and P_N:

$$J(\boldsymbol{q}) = \frac{\partial \boldsymbol{f}}{\partial \boldsymbol{q}^T} \quad . \ . \ . \ . \ . \ . \ . \ . \ . \ . \ . \ . \ . \ . \ (6)$$

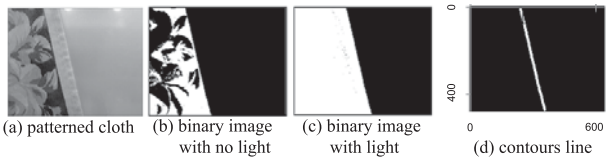

(a) patterned cloth (b) binary image with no light (c) binary image with light (d) contours line

Fig. 7. Extraction of contour line of patterned cloth.

the following calculation is repeated:

$$\boldsymbol{q_{t+1}} = \boldsymbol{q_i} + J^+(\boldsymbol{q})(\boldsymbol{P}_1 - \boldsymbol{P}_{N,t}) \quad . \ . \ . \ . \ . \ . \ . \ (7)$$

$$\boldsymbol{P}_t = \boldsymbol{f}(\boldsymbol{q}_t) \quad . \ . \ . \ . \ . \ . \ . \ . \ . \ . \ . \ . \ . \ . \ (8)$$

Contour shapes are corrected by determining θ_i satisfying the following equation:

$$\min ||\boldsymbol{P}_1 - \boldsymbol{P}_{N,t}|| \leq \alpha \quad . \ . \ . \ . \ . \ . \ . \ . \ . \ . \ (9)$$

Here, α is set to be an infinitesimally small value. $J^+(\boldsymbol{q})$ is a pseudo inverse matrix of $J(\boldsymbol{q})$ and equals $J^T(\boldsymbol{q})(J(\boldsymbol{q})J^T)^{-1}$. Contour lines obtained by adjusting deflection angles at each node to converge at the starting point P_1 and the end point P_N are hereinafter referred to as converged shapes.

4. Experiment

4.1. Contour Extraction

Experiments were conducted to see if contour lines could be extracted from patterned cloth. The thickness of the cloth was 0.16mm, and the hem was thicker by 0.4 mm. **Fig. 7(a)** is a sensor image with an irradiation intensity of the liquid crystal display of 0 cd/m^2. It was taken when the fingers pinched, leaving no gaps, the edge of the cloth. The binary image in this case is in **Fig. 7(b)**. Regions of the object and background were not divided because the pattern had high contrast around the object contours. The binary image at an irradiation intensity of the liquid crystal display of 226 cd/m^2 is shown in **Fig. 7(c)**. The effects of the pattern around the contours were suppressed and regions were divided. The coordinate string obtained by tracing boundary pixels between the object and background is shown in **Fig. 7(d)**. Similar experiments acquiring contour coordinate strings were done on pieces of cloth having different patterns.

Corner edges of cloth were identified based on curvature θ_i determined from the coordinate strings of contours. Using parameters for curvature calculation of $\varsigma = 50$ pixel and $\alpha = 0$ pixel, curvature points satisfying $30 \leq \theta_i \leq 150$ deg are considered to be candidates for corner edges. If there are multiple candidate points in neighboring pixels, the point with the highest θ_i in the range of 50 pixel is detected as a corner edge. With the fingers pinching and identifying 30 points on a straight contour and 4 corner edges, a success rate of 96% was obtained. The rucks of cloth and irregularities in contour lines in the case of pile fabric made it clear that how to set the parameters for

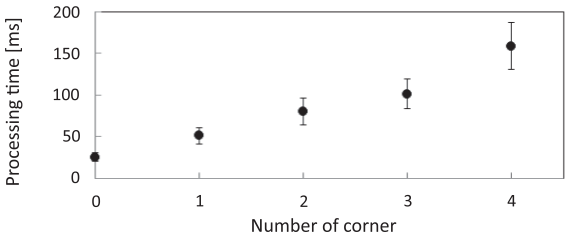

Fig. 8. Processing time required to acquire local contour information.

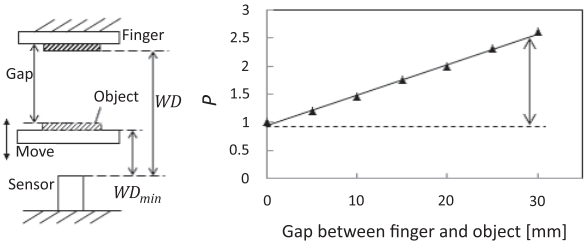

Fig. 9. Relationship between gaps and change coefficient of dimensions ρ when object is pinched.

the curvature calculation and how to adjust the width of the grip are issues yet to be solved. In addition, due to intensified light transmitted through the gaps, image processing is necessary to extract contours and remove noise if the fabric is open weave.

The processing time required from the input of an image to the acquisition of local contour coordinate strings is shown in **Fig. 8**. The processing time was 25 ms when there were no corner edges and 50 ms when there were. Calculation time increased with the number of candidate points in neighboring pixels and the number of corner edges detected.

4.2. Acquisition of Developed Shapes

The distance from the sensor to an object changes when there is a large gap between the finger pad and the pinched object. Assuming the working distance when the object is pinched with no gaps is WD, the shortest working distance when there is a gap is WD_{min}, and dimensions determined through the image measurement are L and L_{max}, the change coefficient of the dimensions is expressed as follows:

$$\rho = \frac{L_{max}}{L} \quad \cdots\cdots\cdots\cdots\cdots\cdots \quad (10)$$

The relationship between gaps and ρ is shown in **Fig. 9**. ρ was obtained by performing image calculation for the length of sample sides with different distances from the sensor to the object. $\rho = 1$ when an object is pinched with no gaps, but the wider the grip width g_w is compared to the width of the object, the larger the deviation from dimensions is. In this study, the grip width g_w is predetermined so that the finger pad of the grip lightly touches the object while tracing its contours.

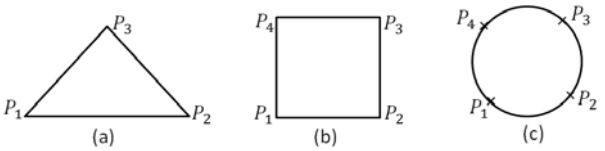

Fig. 10. Developed shapes of cloth: P_i is regrasping position.

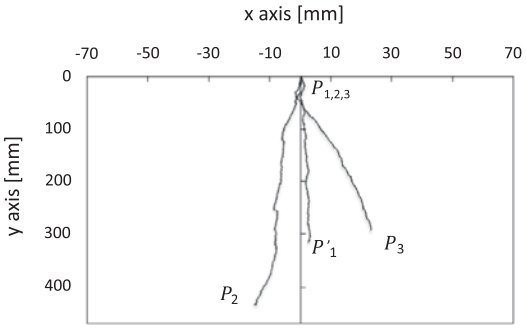

Fig. 11. Contour coordinate obtained through tracing.

Table 1. Comparison of lengths of each side and measured values.

	Length of side [mm]		
	$\lvert\overline{P_1P_2}\rvert$	$\lvert\overline{P_2P_3}\rvert$	$\lvert\overline{P_3P'_1}\rvert$
actual shape	460	330	330
ς=200	443	324	304

In an experiment, developed shapes were extracted from local contour coordinate strings for pieces of cloth with a thickness of 0.89 mm and a stiffness of 30 mm, as shown in **Fig. 10**. Here, stiffness is the average value of the textile in the lateral and longitudinal directions measured using the cantilever method of JIS L1096 [17]. The hanging hand lifted the cloth at around P_1 while the tracing hand traced the edge of the suspended cloth downward starting from P_1. Regrasping motions were carried out at $P_n\{n = 2 \sim 4\}$ until contours were traced to the end point P_1'. Contours $\Delta P_1P_2P_3$ with vertices P_1, P_2, and P_3, as shown in **Fig. 10(a)**, were traced with a grip width g_w of 2 mm and pinching depth g_h^{ref} of 25 mm. **Fig. 11** shows contour coordinate strings of each side calculated by integrating local contour information. Regrasping motions were carried out at corner edges P_1 and P_2, and all contours of the object were traced. Contour coordinate strings from P_1 to P_2, P_2 to P_3, and P_3 to P_1' were extracted. **Table 1** lists the lengths of each side calculated from pixel coordinates. The maximum deviation in side length was approximately 20 mm. Corner edge angles $\angle P_1P_2P_3$, $\angle P_2P_3P_1'$, and $\angle P_3P_1'P_2$ when ς was 50 or 200 are shown in **Table 2**. Curvature differed depending on the value of ς. The distance from P_1 to P_1' was 188.5 mm and 45.8 mm when ς was 50 and 200, respectively. The developed shape determined from $\angle P_1P_2P_3$ and $\angle P_2P_3P_1'$ is shown in **Fig. 12**. The shape when ς was 50

Table 2. Values of ς and corner angles.

	Angle of corner [deg]			error [mm]
	$\angle P_1P_2P_3$	$\angle P_2P_3P'_1$	$\angle P_3P'_1P_2$	
ς=50	66.5	98.4	54.2	188.5
ς=200	47.1	99.3	50.7	45.8

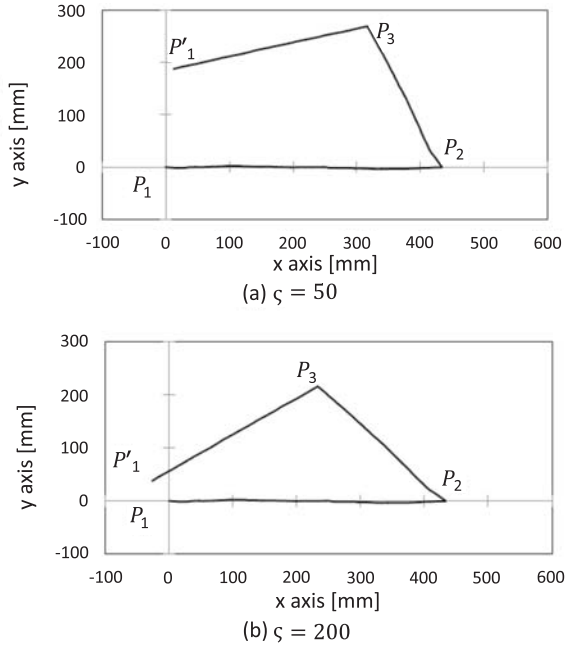

Fig. 12. Developed shape of triangular cloth when ς is 50 or 200.

Table 3. Lengths of side and measured values of angles.

Length of side [mm]			
$\lvert\overline{P_1P_2}\rvert$	$\lvert\overline{P_2P_3}\rvert$	$\lvert\overline{P_3P_4}\rvert$	$\lvert\overline{P_4P'_1}\rvert$
233	193.2	225.9	202.4
Angle of corner [deg]			
$\angle P_1P_2P_3$	$\angle P_2P_3P_4$	$\angle P_3P_4P'_1$	$\angle P_4P'_1P_2$
87.5	96.5	96.4	88.9

was more similar to the actual shape than when ς was 200 owing to smaller positional deviation of P_1 and P'_1. In the same manner, the contours of a 230 mm $\times$ 215 mm piece of cloth with vertices P_1, P_2, P_3, and P_4, as shown in **Fig. 10(b)**, were traced with ς set to 200. The length from P_1 to P_2, P_2 to P_3, P_3 to P_4, and P_4 to the end point P'_1 are shown in **Table 3** along with the curvature at each corner edge. The contour coordinate strings and developed shapes in this case is shown in **Fig. 13**. The length from P_1 to P_2 was 37.1 mm, and the developed shape as a result of tracing was not a closed curve. **Fig. 14** shows the contour coordinate strings and developed shape when the contours of a circular piece of cloth with a diameter of 180 mm were traced with a ς of 200. Because the curvature gradually changed at regrasping points P_2, P_3, and P_4, the contours of the developed shape was curved. As the

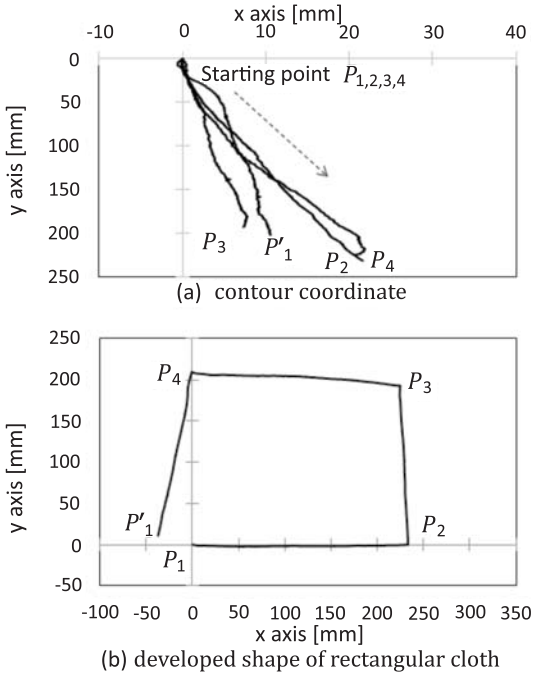

Fig. 13. Contour coordinate strings and developed shape of rectangular cloth.

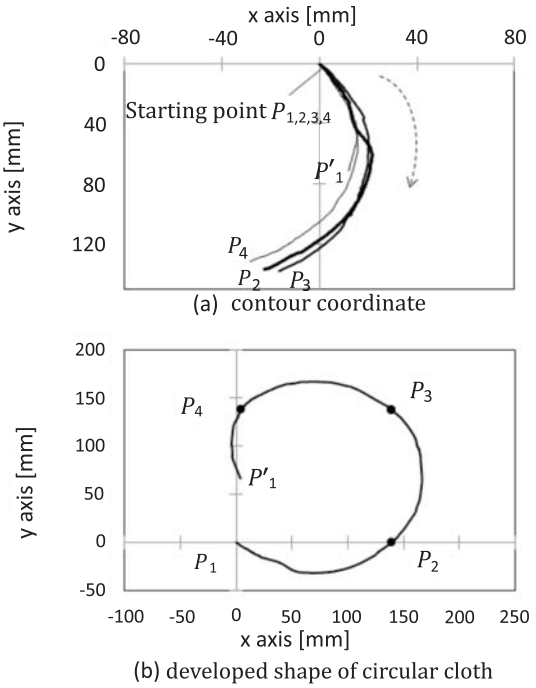

Fig. 14. Contour coordinate strings and shape of circular.

length from P_1 to P'_1 was 66.7 mm, the actual shape was not correctly identified.

4.3. Correction of Developed Shape

Developed shapes were corrected by adjusting the deflection angle q of each node so as to converge the starting point P_1 and the end point P'_1. The corrected result for the developed shape of triangular cloth (**Fig. 12(b)**) is

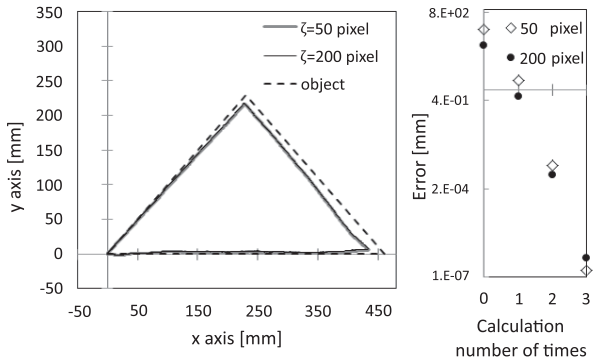

Fig. 15. Results of correction of shape in **Fig. 12(b)**.

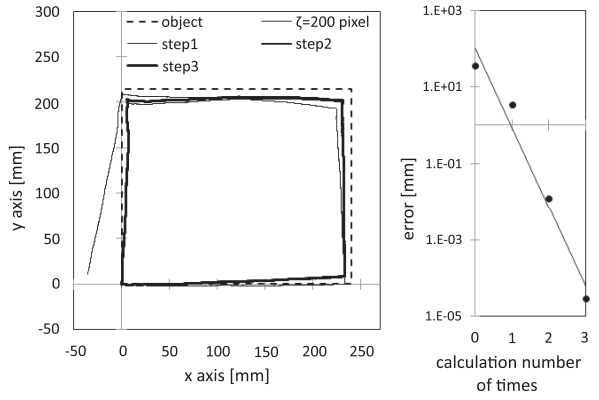

Fig. 16. Results of correction of shape in **Fig. 13(b)**.

shown as a solid line **Fig. 15**. The correction calculation repeated three times produced a distance from P_1 to P_1' of 1.7×10^{-7} mm when ς was 50 and 5.2×10^{-7} mm when ς was 200. The degree of discrepancy between the actual shape shown as a broken line and the developed shape was determined using the following equation:

$$E_H(\boldsymbol{x},\boldsymbol{y}) = \frac{\sum_{i=1}^{n} |x_i - y_i|}{\sum_{i=1}^{n} x_i} \quad \ldots\ldots\ldots \quad (11)$$

$\boldsymbol{x} = (x_1, x_2, \ldots, x_n)^T$ and $\boldsymbol{y} = (y_1, y_2, \ldots, y_n)^T$ are binary vectors for the actual shape and the developed shape, respectively. Regions inside contours are defined as 1, and outside contours are defined as 0. In this study, the two shapes were highly similar when the numbers of contour nodes were the same and $E_H \leq 0.15$. The E_H value of the shape before correction, which was represented by a closed curve by connecting P_1 and P_1', was 0.19, while that of converged shape after correction with a ς of 200 was 0.075. The corrected result for the developed shape of rectangular cloth (**Fig. 13(b)**) is shown in **Fig. 16**. The E_H value of the shape before correction was 0.22. After the correction calculation was used three times, a distance from P_1 to P_1' of 1.5×10^{-7} mm and a E_H value of 0.13 were achieved. The corrected result for the developed

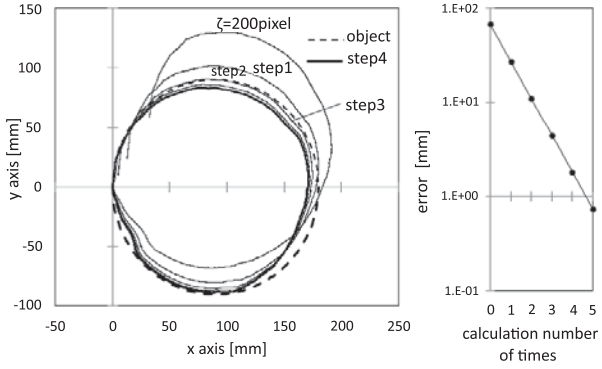

Fig. 17. Results of correction of shape in **Fig. 14(b)**.

shape of a circular piece of cloth (**Fig. 14(b)**) is shown in **Fig. 17**. The shape was corrected by approximating contours using the segments $\overline{P_1P_2}$, $\overline{P_2P_3}$, $\overline{P_3P_4}$, and $\overline{P_4P_1'}$. The E_H value of the shape before correction was 0.39. After the correction calculation was used three times, the distance from P_1 to P_1' of 0.74 mm and the E_H value of 0.052 were achieved.

The degree of discrepancy E_H was significantly reduced by automatically adjusting the deflection angles of each node of the contour so as to converge the starting point and the end point. In addition, for pieces of cloth with different thicknesses and materials, E_H values of 0.15 or less were obtained to the acquire shapes similar to actual shapes. On the other hand, when contours were corrected through direct approximation, as in the case of circular objects, discontinuous curves were sometimes obtained. An increase in adjusted deflection angles should be examined in such cases.

In our experiments, the grip width was set to approximately double the thickness of the cloth when contours were traced. For clothes, with the thickness of the cloth changing at the edges, the value of g_w was equal to or smaller than c_{th}, and contour tracing failed.

5. Conclusion

In this paper, a method of acquiring developed shapes by actively searching for contours of cloth using an image sensor embedded in the finger pad of a robot was proposed. Experiments were performed to acquire shapes that integrated local contour information and to correct the shapes of materials, and the results indicated the effectiveness of this method. Future issues are the following: 1) automatic adjustment for grip width corresponding to changes in cloth thickness, 2) contour tracing for tubular cloth assuming clothes, and 3) form recognition using developed shapes and partial contour shapes.

References:

[1] J. K. Parker, R. Dubey, F. W. Paul, and R.j. Becker, "Robotic Fabric Handling for Automation Garment Manufacturing," Trans. of ASME J. of Engineering for Industry, Vol.105, pp. 21-26, 1983.

[2] E. Torgerson and F. W. Paul, "Vision Guided Robotic Manipulation for Apparel Manufacturing," Proc. 1987 IEEE Int. Conf. on Robotics and Automation, Vol.2, pp. 1196-1202, 1987.
[3] G. J. Monkman, "Robot Grippers for Use with Fibrous Materials," Int. J. of Robotics Research, Vol.14, No.2, pp. 144-151, 1995.
[4] N. Fahantidis, et al., "Robot handling of Flat Textile Materials," IEEE Robotics and Automation Magazine, pp. 34-41, 1997.
[5] K. Paraschidis, et al., "A Robotic System for Handling Textile Materials," Proc. IEEE Int. Conf. on Robotics and Automation, Vol.3, pp. 1769-1774, 1995.
[6] P. M. Taylor (Eds.), "Sensory Robotics for the Handling of Limp Materials," pp. 3-138, Springer-Verlag, 1990.
[7] E. Ono, N. Kita, and S. Sakane, "Strategy for unfolding a fabric piece by cooperative sensing of touch and vision," Proc. IEEE Int. Conf. on Intelligent Robots and Systems, pp. 441-445, 1995.
[8] S. Hata, J. Hayashi, H. Hojoh, and T. Hamada, "Design of Cloth Handling Robot System," IEEE Int. Conf. on Industrial Technology, pp. 1611-1616, 2010.
[9] K. Salleh, H. Seki, Y. Kamiya, and M. Hikizu, "Tracing Manipulation in Clothes Spreading by Robot Arms," J. of Robotics and Mechatronics, Vol.18, No.5, pp. 564-571, 2006.
[10] Dynamic Folding of a Cloth with Two High-speed Robot Hands and Two High-speed Sliders, 2011 IEEE Int. Conf. on Robotics and Automation, pp. 5486-5491, 2011.
[11] Y. Kita, T. Ueshiba, E. S. Neo, and N. Kita, "A method for handling a specific part of clothing by dual arms," Proc.IEEE Int. Conf. on Intelligent Robots and Systems, pp. 4180-4185, 2009.
[12] K. Hamajima and M. Kakikura, "Planning Strategy for Task Untangling Laundry – Isolating Clothes from a Washed Mass –," J. of Robotics and Mechatronics, Vol.10, No.3, pp. 244-251, 1998.
[13] Y. Sugiura, T. Igarashi, H. Takahashi, T. A. Gowon, C. L. Fernando, M. Sugimoto, and M. Inami, "Graphical Instruction for A Garment Folding Robot," ACM SIGGRAPH 2009 Emerging Technologies, 2009.
[14] K. Hamajima and M. Kakikura, "Planning Strategy for Task Untangling Clothes – Classification of Clothes –," J. of Robotics and Mechatronics, Vol.12, No.5, pp. 577-584, 2000.
[15] F. Osawa, H. Seki, and Y. Kamiya, "Unfolding of Massive Laundry and Classification Types by Dual Manippulator," J. of Advanced Computational Intelligence and Intelligent Informatics, Vol.11, No.5, pp. 457-463, 2007.
[16] F. Osawa and K. Kanou, "Contour Tracking of Soft Sheet Materials using Local Contour Image Data," Int. J. of Automation Technology, Vol.6, No.5, pp. 654 - 661, 2012.
[17] JIS L 1096, "Testing methods for woven and knitted fabrics."

Name:
Fumiaki Osawa

Affiliation:
Department of Electrical and Electronic Engineering, Daido University

Address:
10-3 Takiharu-cho, Minami-ku, Nagoya 457-8530, Japan

Brief Biographical History:
2005- Assistant Professor, Faculty of Engineering, Daido Institute of Technology
2009- Associate Professor, Dept. of Electrical and Electronic Engineering, Daido University

Main Works:
• "Control Variables for Food Slicing Supporting Cooking and Improved Operation," Int. J. of Automation Technology, Vol.3, No.6, pp. 751-759, 2009.

Membership in Academic Societies:
• Institute of Electrical Engineers of Japan (IEEJ)
• Japan Society of Precision Engineering (JSPE)

Name:
Kazunori Kanou

Affiliation:
Department of Electrical and Electronic Engineering, Daido University

Address:
10-3 Takiharu-cho, Minami-ku, Nagoya 457-8530, Japan

Main Works:
• "Contour Tracking of Soft Sheet Materials Using Local Contour Image Data," Int. J. of Automation Technology, Vol.6, No.6, pp. 654-661, 2012.

Membership in Academic Societies:
• Institute of Electrical Engineers of Japan (IEEJ)

Name:
Yasushi Yamada

Affiliation:
Department of Electrical and Electronic Engineering, Daido University

Address:
10-3 Takiharu-cho, Minami-ku, Nagoya 457-8530, Japan

Brief Biographical History:
1984 Received B.S. degree from Shizuoka University, Japan
1986 Received M.S. degree from Shizuoka University, Japan
1986- Toyota Central Research and Development Laboratories, Inc., Japan
2004 Received Ph.D. degree from Shizuoka University, Japan
2011 Joined the Department of Electrical and Electronic Engineering, Daido University, Japan

Main Works:
• "Thermal characterization of Cu nanoparticle joints for power semiconductor device," Microelectronics Reliability, Vol.53, pp. 1543-1547, 2013.

Membership in Academic Societies:
• Institute of Electrical Engineers of Japan (IEEJ)
• Japan Institute of Electronic Packaging (JIEP)